Available online at www.sciencedirect.com
ScienceDirect
Physics Letters A 369 (2007) 518–523
PHYSICS LETTERS A
www.elsevier.com/locate/pla

Engineering the bandgap of a two-dimensional photonic crystal with slender dielectric veins

Wen-Long Liu *, Tzong-Jer Yang

Department of Electrophysics, National Chiao Tung University, Hsinchu 30050, Taiwan, ROC

Received 21 December 2006; received in revised form 22 March 2007; accepted 7 May 2007

Available online 23 May 2007

Communicated by J. Flouquet

Abstract

This study proposes the double-hybrid-rods structure of two-dimensional (2D) photonic crystals of a square lattice. A square dielectric rod connected with slender rectangular dielectric veins on the middle of each side of dielectric square rod. Some specific modes are found to be sensitive to certain structural parameters, such as the length, the dielectric constant and the shift of the position of the veins, etc., and giving rise to a new complete PBG at lower index bands. These results could be understood by the use of band structure point of view. In particular, by carefully adjusting the structural parameters, the band structure of the photonic crystal can be substantially engineered to achieve large bandgaps.

PACS: 42.70.Qs; 42.25.Bs; 41.20.-q

Keywords: Photonic band gap; Photonic crystals; Band structure

Since the pioneering works of Yablonovitch and John in 1987 [1,2], photonic crystals (PCs) are now a fascinating issue of research. PCs are of artificial materials having the periodical modulation of dielectric structures in space and there exist photonic band gaps (PBGs) in which the propagation of electromagnetic (EM) waves in any propagating direction and polarization state is inhibited. A PBG can lead to various peculiar physical phenomena [3] and providing potential applications [4–6]. The wider a PBG is, the greater the forbidden region of the frequency spectrum. Thus, the search for photonic crystals that possess wider band gaps is an important issue. Various methods for creating large PBGs or in increasing an existing PBG by altering the dielectric constant $\epsilon(\mathbf{r})$ within a unit cell, have been proposed. These methods include rotating the lattices [7], using anisotropic dielectric materials [8], rotating the noncircular rods [9–11], and modifying the permittivity distribution in a unit cell [12,13]. Some research groups have successfully fabricated PCs by holographic lithography [14] that can yield two- and three-dimensional (3D) complete PBGs [15,16]. Several PC structures consisting of rods, spheres or cubes linked by dielectric veins as a completely closed 2D or 3D structures would give a large complete band gap [17–19]. In addition, the search for 3D PBG structures based on a non-close-packed face-centered cubic lattice of spherical shells connected by thin cylindrical tubes was proposed [20]. More recently, it was demonstrated that a 2D PBG structures with open veins can also remarkably increase complete PBG [21].

This study proposes the double-hybrid-rods structure of 2D PCs by placing slender rectangular dielectric veins on the middle of each side of square rod in each unit cell. There exists one complete photonic band gap (PBG) in higher frequency band of the prototype square lattices with only square rods [22]. When extending the dielectric veins, some specific modes are found to be sensitive to certain structural parameters, such as the length, the dielectric constant and the shift of the position of the veins, etc. Then, this PBG disappears and for a proper value of vein length another complete PBG at lower index bands opens. The variation of bands near the PBG's boundaries can be interpreted by considering the effects of scattering and interference of EM waves to be significantly modified and enhanced when intro-

* Corresponding author.
E-mail address: wlliuz@ms48.hinet.net (W.-L. Liu).

0375-9601/$ – see front matter
doi:10.1016/j.physleta.2007.05.045

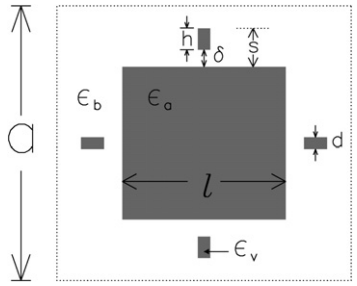

Fig. 1. Schematic diagram of the proposed photonic crystals. The square dielectric rod with a side-length l and dielectric ϵ_a is placed in air with $\epsilon_b = 1.0$ at the center of a 2D square lattice with a lattice constant, a, in the xy-plane. Another dielectric vein with $\epsilon = \epsilon_v$ and length h and width d is inserted in each unit cell on the middle of each side of dielectric square rod, forming composite lattices. The shift length s of the inserted vein is defined with respect to the edge of the square rod, where δ is the crevice between the edges of the square rod and the vein, thus s is denoted by $s = \delta + h$.

ducing the extra dielectric veins into each unit cell. In this study, we want to understand these effects by the use of band structure point of view. When the length of veins increases, the wavelength of resonance mode would increase too. That is the resonance frequency would decrease. Generally, the EM-field distributions bear strong resemblances to electronic orbitals and, like their electronic counterparts, could lead to bonding and anti-bonding interactions between neighboring rods [23]. The relevance (the strength) of the interactions among scattering rods is attributed to the field distribution characteristics. In terms of band structure terminology, the band center of the band reflects the resonance frequency and the band width reflects the relevance (the strength) of the interactions or the EM-field distribution characteristics among scattering rods. In this PC, the structural parameters are properly chosen so that the photonic band structure can be optimized. Although this proposal is similar to Ref. [21] mentioned in the preceding paragraph, it has an advantage that enables us to more precisely design the band structures by utilizing additional arbitrary parameters (the dielectric constant and the shift of the position of the veins), and hence it will prove useful in designing PBGs of a variety of photonic crystals.

Fig. 1 displays the schematic diagram of the proposed PC structure. The square dielectric rod with a side-length of l and dielectric ϵ_a is placed in air background with $\epsilon_b = 1.0$ at the center of a 2D square lattice with a lattice constant, a, in the xy-plane. Another dielectric vein with $\epsilon = \epsilon_v$, length h and width d is placed in each unit cell on the middle of each side of the dielectric square rod, forming composite lattices. The term δ is the crevice between the edges of square rod and vein. The shift length s is thus given by $s = \delta + h$. The following parameters were used in the calculations: $\epsilon_a = 11.4$ appropriate for gallium arsenide (GaAs) at wavelength $\lambda \approx 1.5$ μm and $\epsilon_b = 1.0$ in air. In our calculations, the band structures of the PCs were calculated using the plane-wave expansion method, described in detail in the literature [24–26]. The Fourier expansion with 625 plane waves was used to calculate the PBGs for the E/H-polarization (in-pane magnetic/electric fields) and the convergence accuracy for the several lowest photonic bands was better than 1%. This study explored the influence of the slender dielectric veins on the 2D complete PBG. As an example, three cases of the dielectric constant of veins ϵ_v were considered, with $\epsilon_v = 6$, 11.4 and 16. First, the PBG structures of the prototype square lattices with only square rods were calculated, as shown in Fig. 2(a), the side-length of square rod fixed at $l = 0.57a$. The solid (dotted) curves correspond to the E (H)-polarization. The diagram clearly shows that a complete PBG exists at higher index bands resulting from the superposition of the $E8$–9 and $H6$–7 gaps. If the square rods are linked with dielectric veins at each middle side of the square rods, the influences of the length h of the dielectric vein on the PBGs is now investigated. The calculated band structures for three choices of the dielectric constant of veins are demonstrated in Fig. 2(b) as $\epsilon_v = 6$, (c) $\epsilon_v = 11.4$ and (d) $\epsilon_v = 16$, respectively. The dielectric vein has a width of $d = 0.08a$, and a crevice of $\delta = 0$ between the edges of vein and square rod.

We find that the higher complete PBG shown in Fig. 2(a) disappears in Figs. 2(b)–(d) and another complete PBG at lower index bands opens while the length of veins continues to increase. For $\epsilon_v = 6$ the overlap of the $H2$–3 band gap and the far wider $E3$–4 band gaps creates a complete PBG, with the band edges lying at the **M** symmetry point. On increasing the vein length substantially lowers the frequency of **M** symmetry point of $H2$ band. The same happens when ϵ_v increases from 6 to 16. Consequently, the **M** point is lower than the **Γ** point somewhere for the case of $\epsilon_v = 11.4$ and $\epsilon_v = 16$, and then this complete PBG is bounded on the lower side by the **Γ** point of $H2$ band. On the other hand, the top edge of this complete PBG remains unchanged and lies at **M** point of $H3$ band. When it reaches ϵ_v=16 and $h = 0.19a$, the **Γ** point of $E4$ band is below than the **M** point of $H3$ band; thus the complete PBG is bounded on the upper side by the **Γ** point of $E4$ band. Comparison with the variation of complete PBG boundaries of Figs. 2(b)–(d) shows that the lower boundary first shifts downwards, then remains unmodified. While the upper boundary first remains unchanged, then moves downwards. It is clearly seen that the largest complete PBG occurs at $h = 0.215a$, namely, the veins are fully connected at the lattice unit cell boundary for the case $\epsilon_v = 6$. However the complete PBG reaches its maximum width with midgap frequency $\omega_g = 0.42385(2\pi c/a)$ and the gap size $\Delta\omega = 0.0557(2\pi c/a)$ at the intermediate value of $h = 0.19a$ for the case $\epsilon_v = 11.4$, and then remains unchanged where $h = 0.215a$. Here c is the light speed in vacuum. In particular, for $\epsilon_v = 16$ increasing h from $0.155a$ to $0.19a$, we find that both the lower and upper boundaries shift towards lower frequencies. The lower boundary of this complete PBG (i.e., the lower band edge of the H-polarized gap) moves a bit faster than the upper boundary (i.e., the upper band edge of the E-polarized gap); therefore, this complete PBG becomes wider. If h continues to increase and reaches $0.215a$, the complete PBG shrinks again.

What is the key factor that leads to lower band edges at certain symmetry points and hence create a gap when the square dielectric rod is connected with slender dielectric veins? In order to clarify this issue, we calculate the spatial energy distribution for the corresponding states. Figs. 3(a)–(c) plot the

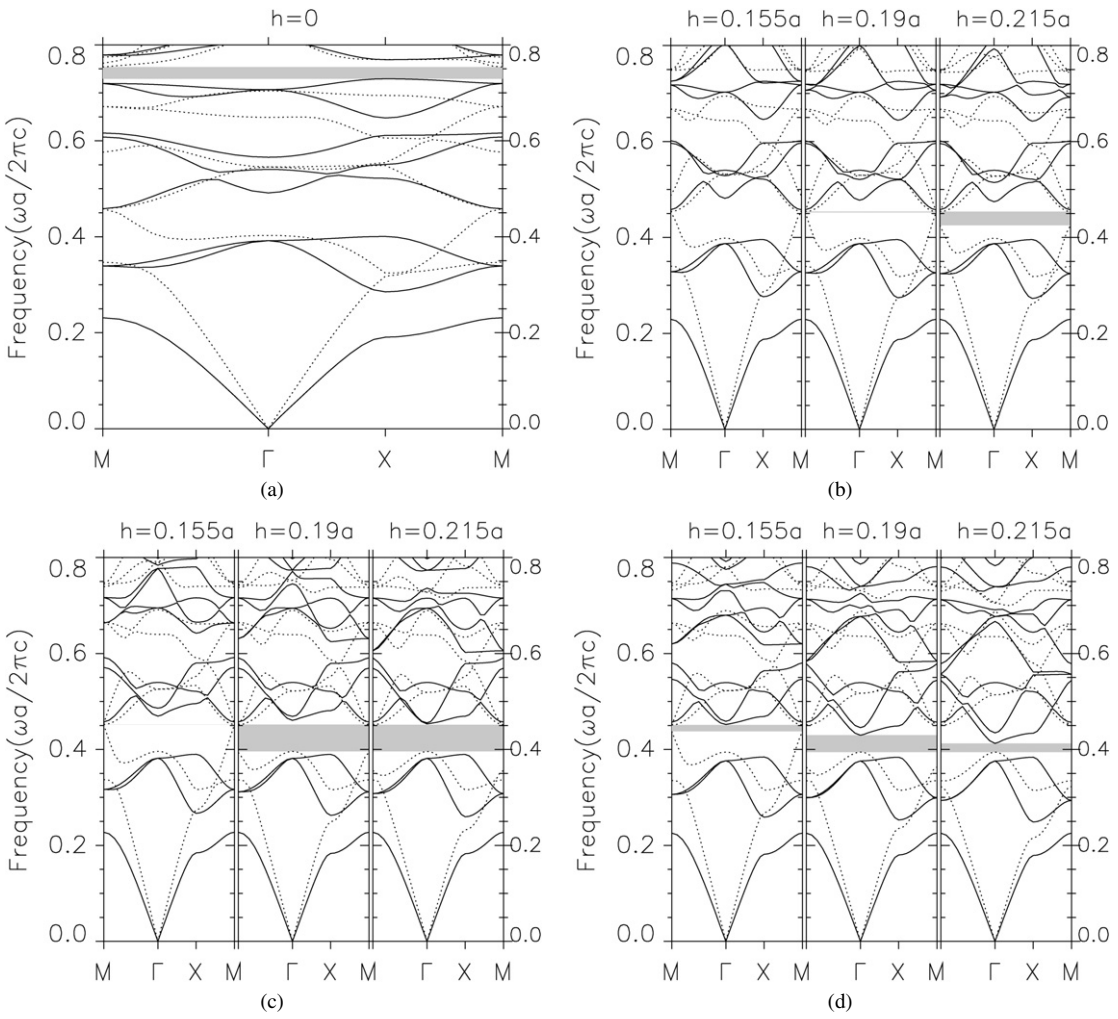

Fig. 2. Photonic band structures for two structures: the prototype structure without the inserted veins for fixing the side-length of square rod at $l = 0.57a$, $\epsilon_a = 11.4$, appropriate for GaAs material; $\epsilon_b = 1.0$ in air as shown in (a) and three choices of the dielectric constant of veins are demonstrated in (b) $\epsilon_v = 6.0$, (c) $\epsilon_v = 11.4$, (d) $\epsilon_v = 16.0$. The other parameters are the same as those in (a) except for parameters of veins: $\delta = 0$, $d = 0.08a$ and h: $0.155a$ (left panel), $0.19a$ (middle panel), $0.215a$ (right panel). The solid and dotted curves correspond to the E- and H-polarizations, respectively. The gray area marks the complete gap region.

spatial distributions of the electric field intensity $|E^2|$ within a unit cell of the PC at the **M** point of (a) $H2$ band (or denoted by $H^{(2,M)}$) for $h = 0$, (b) $H4$ band ($H^{(4,M)}$) for $h = 0$, and (c) $H2$ band ($H^{(4,M)}$) for $\epsilon_v = 6$ and $h = 0.215a$. Here we mark the states in accordance with their ordering in frequency for the prophase, namely, the initial mode $H^{(n,M)}$ denotes the nth band for the H-polarization mode at **M** point. When $h = 0$ it is apparent that the spatial $|E^2|$ distributions of the $H^{(2,M)}$ mode always concentrates inside the square rod, exhibiting a single parallelogram-like spot; on the contrary, the high index mode ($H^{(4,M)}$) possesses four spots close to the edges of square rod. While the square dielectric rod is connected with slender dielectric veins, the $|E^2|$ distribution of $H^{(4,M)}$ mode in the unit cell will spread out from square rod and concentrate inside the dielectric veins, then leads to the shift of frequencies of $H^{(4,M)}$ mode; consequently, the $H^{(4,M)}$ mode is below the $H^{(2,M)}$ and $H^{(3,M)}$ modes. Fig. 3(c) plots the spatial $|E^2|$ distribution of $H^{(4,M)}$ mode (corresponding to the **M** point of $H2$ band shown in the right panel of Fig. 2(b)). The energy distributions for other modes of certain symmetry points at band edges are also investigated, and the same phenomenon is observed. It is worth pointing out that field is more spreading out from the square rod owing to extending the vein length.

Figs. 3(d) and 3(e) plot the band center (BC) and band width (BW) versus vein length for $H2$ band with $\epsilon_v = 6$, 11.4, 16 and $E4$ band with $\epsilon_v = 6$; the other parameters are as those in Fig. 2. The curves of BC for $H2$ band in Fig. 3(d) exhibit a plateau profile with slightly sloping at the beginning of curves, and then decline rapidly to their minimum values with 0.372, 0.356 and $0.354(2\pi c/a)$ in turn at a certain h, depending on ϵ_v. The BC of $H2$ band falls off and so the complete PBG occurs (owing to $H^{(4,M)} < H^{(2,M)}$ (or $H^{(3,M)}$)). It can be understood here that the resonance frequency would decrease. Clearly, it is also seen that the curves exhibit another plateau profile at the end of curves (owing to $H^{(4,M)} < H^{(2,\Gamma)}$), except for the solid one with $\epsilon_v = 6$. In the same figure, the BC curves of $E4$ band for $\epsilon_v = 16$ is shown. Notably, the BC curve of $E4$ band decline monotonically to its minimum value around $0.456(2\pi c/a)$ when dielectric veins are fully connected ($h = 0.215a$). The curves of BW for $H2$ band of $\epsilon_v = 6$, 11.4

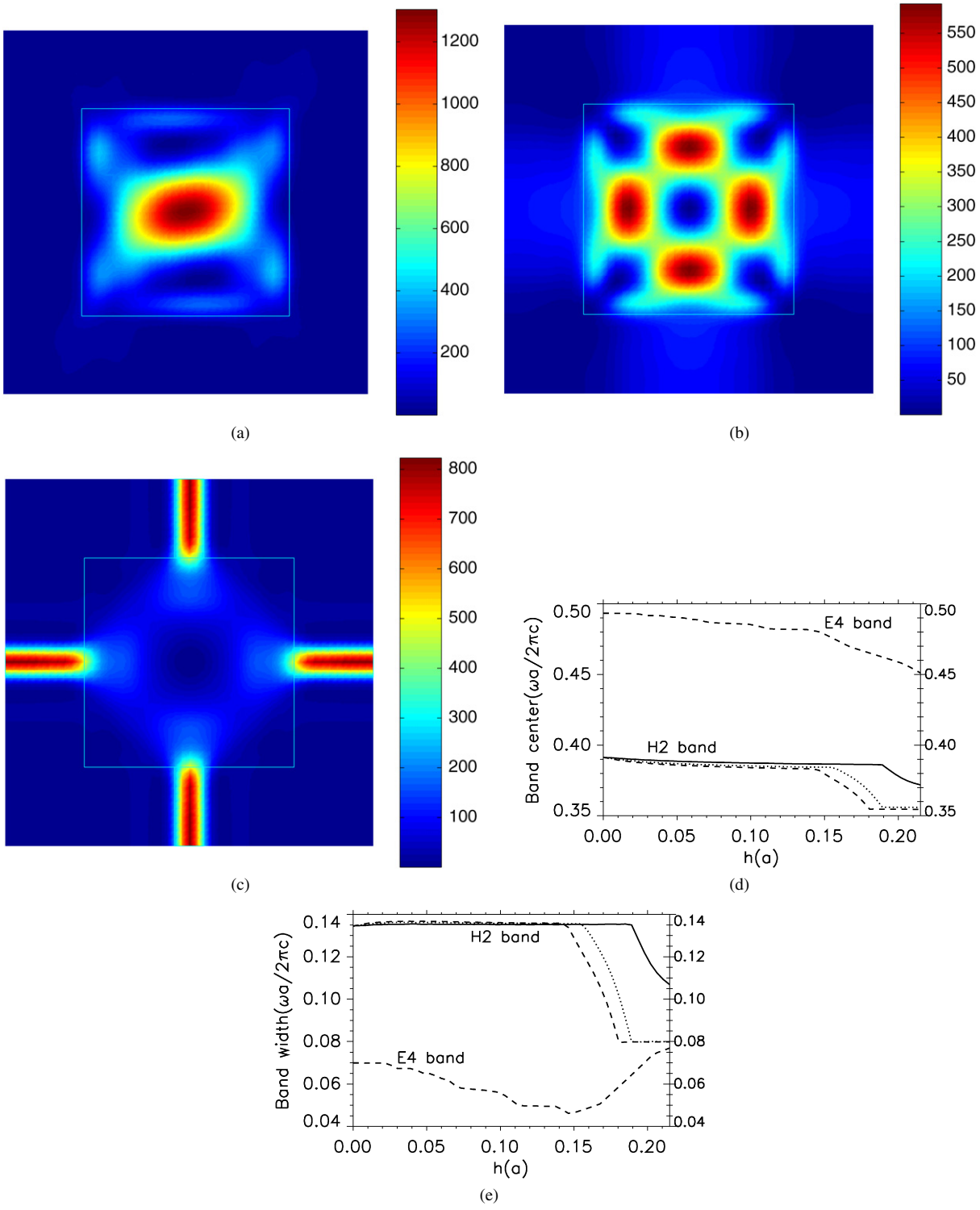

Fig. 3. The spatial distributions of the electric field intensity $|E^2|$ at the **M** point of (a) $H2$ band (or denoted by $H^{(2,M)}$) for $h = 0$, (b) $H4$ band ($H^{(4,M)}$) for $h = 0$, and (c) $H2$ band ($H^{(4,M)}$) for $\epsilon_v = 6$ and $h = 0.215a$. Here we mark the states in accordance with their ordering in frequency for the prophase, namely, the initial mode $H^{(n,M)}$ denotes the nth band for the H-polarization mode at **M** point. The band center (d) and the band width (e) as functions of h for $H2$ band with $\epsilon_v = 6$ (solid line), 11.4 (dotted line), 16 (dashed line) and $E4$ band with $\epsilon_v = 16$.

and 16 versus h are shown in Fig. 3(e). Apparently, all of the BW curves of $H2$ band exhibit a similar profile to the corresponding BC curves. However, they have same value of BW in the flat region at around $0.135(2\pi c/a)$ and $0.08(2\pi c/a)$, respectively. Its existence shows that the BW is insensitive to the extension of dielectric veins. However, the curves of BW with a sharp slant because the $H^{(4,M)}$ mode (i.e., the mode of top band edge of $H2$ band lying at **M** point) is sensitive to the extension of dielectric veins. Besides, this means that field energy is more spreading out from the square rod. The BW curves of

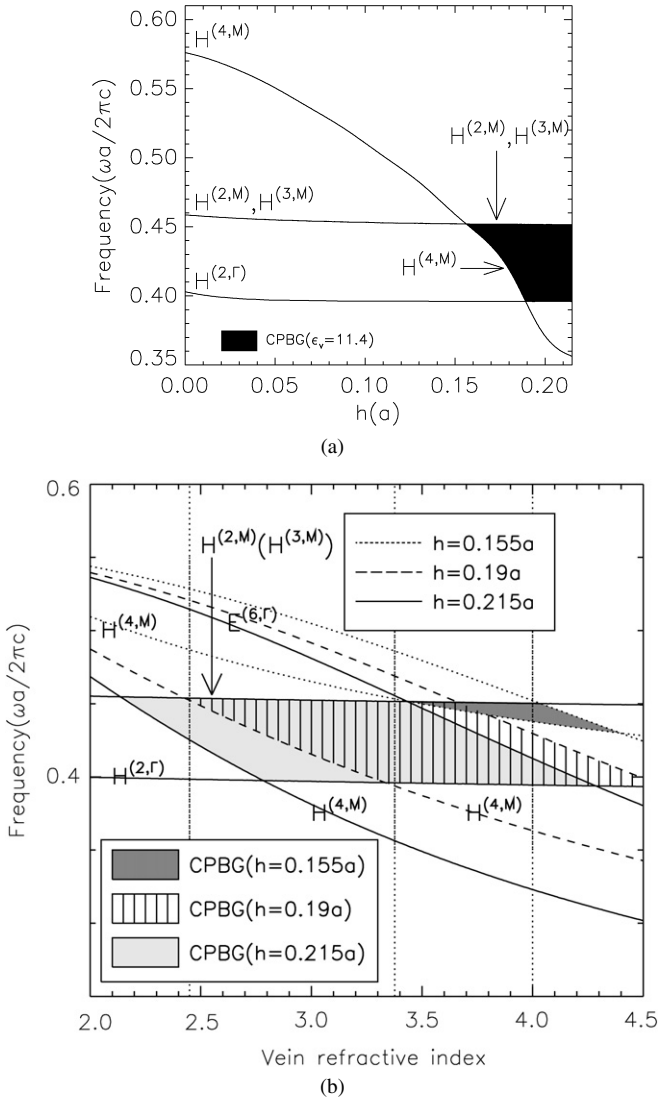

Fig. 4. The positions of the edge states of the lower complete PBG (CPBG): (a) the evolution of the edge states of the lower complete PBG as a function of vein length, h, for $\epsilon_v = \epsilon_a = 11.4$. The other parameters are: $\epsilon_a = 11.4$, $l = 0.57a$, $\delta = 0$ and $d = 0.08a$. The dark region indicates the complete PBG. $H^{(n,\Gamma)}$ ($E^{(n,\Gamma)}$) denote the nth band for the $H(E)$-polarization modes at $\mathbf{\Gamma}$ point. (b) The evolution of the edge states of the lower complete PBG as functions of the vein refractive index for three different vein lengths ($h = 0.155a$, $0.19a$, and $0.215a$). The vein refractive index of $n = 2.45$, 3.376 and 4.0 (i.e., $\epsilon_v = 6.0$, 11.4 and 16.0) are indicated by the vertical dotted lines. The dashed–dotted lines represent the curves of $H^{2,M}$ ($H^{3,M}$) or $E^{2,\Gamma}$ modes for different h values.

$E4$ band ($\epsilon_v = 16$) is also shown in this figure. Here, we have mostly paid attention to the curve of $E4$ band for which the complete PBG is bounded when $h > 0.155a$. It is clearly seen that the BW curve mount up soon from 0.046 to $0.076(2\pi c/a)$ in this region ($h > 0.155a$) because the $E^{(6,\Gamma)}$ mode (i.e., the mode of bottom band edge of $E4$ band lying at Γ point) downshifts to the lower frequency, and thus the field energy is more spreading out from the square rod.

To get better insight into superior features of the hybrid structure, we investigate in detail the edge states of the complete PBGs. Here we will address the lower complete PBG that form the structure described above. In our case slender dielectric veins play a crucial role in opening the lower complete PBG, therefore we have performed two kind of evolutions. First, we have calculated the positions of edge states of the lower complete PBG for a fixed value of dielectric constant of veins. We examined the PBG structures with only square rods (i.e., $h = 0$) to start with and then varied the value of vein length, h. Second, we have investigated the positions of edge states of the lower complete PBG for three different h values as functions of the index of refraction of the slender dielectric veins. Fig. 4(a) plots the evolution of edge states of the lower complete PBG as functions of the vein length, h, for $\epsilon_a = \epsilon_v = 11.4$. The other parameters are as those quoted in Fig. 2(c) (i.e., $\delta = 0$, $l = 0.57a$, $d = 0.08a$). According to the calculation of the photonic band structures, the edge states of the lower complete PBG are $H^{(2,M)}$, $H^{(3,M)}$, $H^{(4,M)}$ and $H^{(2,\Gamma)}$ modes. While, the $H^{(2,M)}$ and $H^{(3,M)}$ modes are degenerate in the region given by $h = [0, 0.215]a$. The frequencies of these two modes and $H^{(2,\Gamma)}$ remain almost unmodified at around 0.452 and $0.396(2\pi c/a)$ in turn. The frequencies of $H^{(4,M)}$ decrease significantly for increasing h. As the $H^{(4,M)}$ mode is below $H^{(2,M)}$ and $H^{(3,M)}$ modes for $h > 0.155a$, the lower complete PBG is opened, and its width increases quite sharply. In the region $h > 0.155a$, the complete PBG is bounded on the lower side by the $H^{(4,M)}$ boundary, and on its upper side by the $H^{(2,M)}$ or $H^{(3,M)}$ boundary. Furthermore, the vein length increases up to about $h = 0.19a$, the $H^{(4,M)}$ mode is again lower than $H^{(2,\Gamma)}$ mode. The complete PBG is thus bounded on the lower side by the $H^{(2,\Gamma)}$ boundary, and on its upper side by the $H^{(2,M)}$ ($H^{(3,M)}$) boundary in the region $h = [0.19, 0.215]a$. Notably, this complete PBG tends to increase in size dramatically in the region $h = [0.155, 0.19]a$, and reaches its maximum value at $h = 0.19a$. Then, the width of this complete PBG remain unmodified.

Fig. 4(b) shows the positions of edge states of the complete PBGs as functions of the vein refractive index (in the range of $2.0 \leqslant n \leqslant 4.5$) for three different length of veins ($h = 0.155a$, $0.19a$, and $0.215a$). Apparently, the appearance of the complete PBGs exhibits a triangle-like outline for $h = 0.155a$ (indicated by the dark gray region) and two parallelogram-like outlines for $h = 0.19a$ (shaded by vertical solid lines) and $h = 0.215a$ (indicated by light gray region). It is seen that the curves of $H^{(2,M)}$ (or $H^{(3,M)}$) and $H^{(2,\Gamma)}$ modes are flat in the region given by $n = [2.0, 4.5]$. However, The $H^{(4,M)}$, $E^{(4,\Gamma)}$ and $E^{(6,\Gamma)}$ modes decrease monotonously for increasing n. For $h = 0.155a$ the bottom edge state is always $H^{(4,M)}$ as $n = [3.43, 4.4]$, while the top edge states of this complete PBG are $H^{(2,M)}$ (or $H^{(3,M)}$) and $E^{(6,\Gamma)}$ modes as $n = [3.43, 4.03]$ and $n = [4.03, 4.4]$ in turn. The maximum width of this gap occurs at $n = 4.03$. For $h = 0.19a$ the complete PBG opens for $n = 2.4$ and closes above $n = 4.5$. When n is increased from 2.4, the top edge states are $H^{(2,M)}$ (or $H^{(3,M)}$) modes, while the bottom edge state is $H^{(4,M)}$ mode. As $n > 3.33$ the $H^{(4,M)}$ mode is below the $H^{(2,\Gamma)}$ mode, thus the complete PBG is bounded on the lower side by the $H^{(2,\Gamma)}$ mode. Meanwhile, the $E^{(6,\Gamma)}$ mode is below the $H^{(2,M)}$ ($H^{(3,M)}$) mode for $n > 3.65$, and hence the complete PBG is bounded on the upper side by the $E^{(6,\Gamma)}$ mode. For $h = 0.215a$, the edge states are the same as those

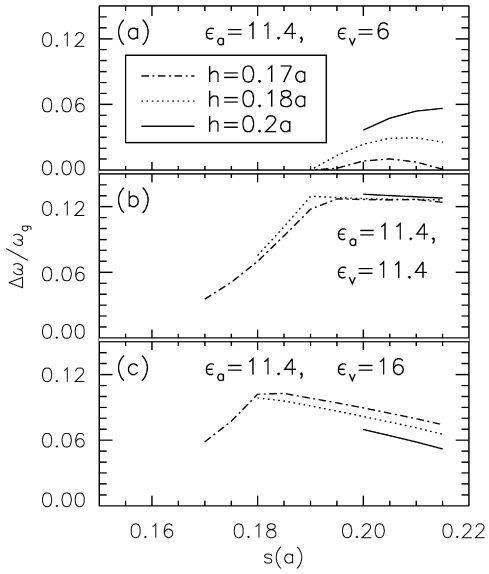

Fig. 5. Variations of $\Delta\omega/\omega_g$ with the shift length s for different vein lengths h: $0.17a$, $0.18a$ and $0.2a$ for (a) $\epsilon_v = 6.0$, (b) $\epsilon_v = 11.4$ and (c) $\epsilon_v = 16.0$. The other parameters are $\epsilon_a = 11.4$, $l = 0.57a$ and $d = 0.08a$.

for $h = 0.19a$. However, both left- and right-hand ends of the parallelogram-like outline are shifted toward lower n regime. In this case the complete PBG starts near $n = 2.13$ and ends at about $n = 4.29$. Notably, in the range of $n = [3.33, 3.65]$ for $h = 0.19a$ and $n = [2.78, 3.43]$ for $h = 0.215a$ the complete PBGs remain unchanged or vary a little. Moreover, there exists the equal maximum size of the complete PBG in the overlap region of $n = [3.33, 3.43]$ for $h = 0.19a$ and $0.215a$. This broad profile with large gap size manifests the large freedom in the choice of the structural parameters, which provide the benefit of the facilitated construction of the PCs with a large allowance of tolerance.

The influence of the shift s outward of the veins on dispersion spectrum is demonstrated by the plot of the dependence of $\Delta\omega/\omega_g$ (the gap width to midgap frequency ratio) as a function of s for different h values ($0.17a$, $0.18a$ and $0.2a$) as shown in Fig. 5 for (a) $\epsilon_v = 6.0$, (b) $\epsilon_v = 11.4$ and (c) $\epsilon_v = 16.0$, respectively. The other parameters were also chosen as $\epsilon_a = 11.4$, $\epsilon_b = 1$, $l = 0.57a$ and $d = 0.08a$. The shift length s, is given as the sum of δ and h. The varying region of s is limited, i.e., only from $s = h$ to $s = (a - l)/2$. All $\Delta\omega/\omega_g$ versus s curves appear to exhibit an asymmetric profile in a finite s range. Moreover, the right-hand end of the curve in a larger ϵ_v extends to a wider region of s. For each value of s, $(\Delta\omega/\omega_g)_{h=0.2a} > (\Delta\omega/\omega_g)_{h=0.18a} > (\Delta\omega/\omega_g)_{h=0.17a}$ when $\epsilon_v = 6$; by contrast, $(\Delta\omega/\omega_g)_{h=0.17a} > (\Delta\omega/\omega_g)_{h=0.18a} > (\Delta\omega/\omega_g)_{h=0.2a}$ when $\epsilon_v = 16$. In the lower-ϵ_v, the vein length of $h = 0.2a$ widens the PBG while shifting the vein towards the lattice unit cell boundary (see Fig. 5(a)). All the curves in Fig. 5(b) exhibit a plateau profile at the right-hand end of the curves spanning a finite region of s in which $\Delta\omega/\omega_g$ is insensitive to changes of s. However, the right-hand end of the curves in Fig. 5(c) declines gradually. These results can be understood to be related to the effective dielectric constant of veins in the region of s. In fact, the complete PBGs can be optimized for a right choice of h and s for a given ϵ_v, since the complete PBGs are always governed by the vein dielectric constant and the vein length.

As a conclusion, we have investigated in detail the photonic band structures of 2D square lattices of a square dielectric rod connected with slender rectangular dielectric veins on the middle of each side of dielectric square rod. Properly adjusting the length, dielectric constant and the shift of the position of veins in the unit cell enables the large complete PBG generated from the composite structure to be achieved. Additionally, the large freedom in the choice of the structural parameters which provide the benefit of the facilitated construction of the PCs with a large allowance of tolerance. The PCs can be easily fabricated and operated in the micro-wave region because a is in the order of microwave wavelengths—several mm or cm, and hence it is anticipated to be encouraged in applications to new microwave devices.

Acknowledgements

The authors would like to thank the National Science Council of the Republic of China, Taiwan (Contract No. NSC 95-2119-M-009-029) and the Electrophysics Department, National Chiao Tung University, Taiwan, for their support and to Young-Chung Hsue for his useful discussions.

References

[1] E. Yablonovitch, Phys. Rev. Lett. 58 (1987) 2059.
[2] S. John, Phys. Rev. Lett. 58 (1987) 2486.
[3] S. John, Nature 390 (1997) 661.
[4] K. Sakoda, Optical Properties of Photonic Crystals, Springer, 2001.
[5] J.D. Joannopoulos, R.D. Meade, J.N. Winn, Photonic Crystals—Molding the Flow of Light, Princeton Univ. Press, 1995.
[6] C.M. Soukoulis (Ed.), Photonic Band Gaps and Localization, Plenum, New York, 1993.
[7] C.M. Anderson, K.P. Giapis, Phys. Rev. B 56 (1997) 7313.
[8] Z.Y. Li, B.Y. Gu, G.Z. Yang, Phys. Rev. Lett. 81 (1998) 2574; Z.Y. Li, B.Y. Gu, G.Z. Yang, Eur. Phys. J. B 11 (1999) 65.
[9] X.H. Wang, B.Y. Gu, Z.Y. Li, G.Z. Yang, Phys. Rev. B 60 (1999) 11417.
[10] C. Goffaux, J.P. Vigneron, Phys. Rev. B 64 (2001) 075118.
[11] N. Susa, J. Appl. Phys. 91 (2002) 3501.
[12] R.D. Meade, A.M. Rappe, K.D. Brommer, J.D. Joannopoulos, J. Opt. Soc. Am. B 10 (1993) 328.
[13] X.D. Zhang, Z.Q. Zhang, L.M. Li, C. Jin, D. Zhang, B. Man, B. Cheng, Phys. Rev. B 61 (2000) 1892.
[14] M. Campbell, D.N. Sharp, M.T. Harrison, R.G. Denning, A.J. Turberfield, Nature 404 (2000) 53.
[15] L.Z. Cai, G.Y. Dong, C.S. Feng, X.L. Yang, X.X. Shen, X.F. Meng, J. Opt. Soc. Am. B 23 (2006) 1708.
[16] D.N. Sharp, A.J. Turberfield, R.G. Denning, Phys. Rev. B 68 (2003) 205102.
[17] M. Qiu, S. He, J. Opt. Soc. Am. B 17 (2000) 1027.
[18] M. Maldovan, E.L. Thomas, J. Opt. Soc. Am. B 22 (2005) 466.
[19] R. Biswas, M.M. Sigalas, K.M. Ho, S.Y. Lin, Phys. Rev. B 65 (2002) 205121.
[20] H. B Chen, Y.Z. Zhu, Y.L. Cao, Y.P. Wang, Y.B. Chi, Phys. Rev. B 72 (2005) 113113.
[21] W.L. Liu, T.J. Yang, Solid State Commun. 140 (2006) 144.
[22] C.S. Kee, J.E. Kim, H.Y. Park, Phys. Rev. E 56 (1997) R6291.
[23] M.I. Antonoyiannakis, J.B. Pendry, Phys. Rev. B 60 (1999) 2363.
[24] K.M. Ho, C.T. Chan, C.M. Soukoulis, Phys. Rev. Lett. 65 (1990) 3152.
[25] Z. Zhang, S. Satpathy, Phys. Rev. Lett. 65 (1990) 2650.
[26] K.M. Leung, Y.F. Liu, Phys. Rev. Lett. 65 (1990) 2646.